Chinese Herbal Medicines 11 (2019) 369–378

Contents lists available at ScienceDirect

Chinese Herbal Medicines

journal homepage: www.elsevier.com/locate/chmed

Original Article

Gynura procumbens aqueous extract alleviates nonalcoholic steatohepatitis through CFLAR-JNK pathway *in vivo* and *in vitro*

Ya-yun Liu[a,b,1], Jiao-jiao You[a,1], Wei Xu[a], Ting Zhai[a], Chun-yuan Du[a], Yong Chen[a,*], Feng-mei Han[a,*]

[a] *Hubei Key Laboratory of Biotechnology of Traditional Chinese Medicine, National & Local Joint Engineering Research Center of High-throughput Drug Screening Technology, Hubei University, Wuhan 430062, China*

[b] *Hubei Key Laboratory of Tumor Microenvironment and Immunotherapy, Medical College of China Three Gorges University, Yichang 443000, China*

ARTICLE INFO

Article history:
Received 22 February 2019
Revised 23 April 2019
Accepted 8 May 2019
Available online 1 October 2019

Keywords:
aqueous extract of *Gynura procumbens* (Lour.) Merr.
nonalcoholic steatohepatitis
methionine and choline-deficient diet
CFLAR
lipid metabolism
oxidative stress

ABSTRACT

Objective: The present work was to investigate the protective effects of the aqueous extract of *Gynura procumbens* (GPAE) against nonalcoholic steatohepatitis (NASH) in mice and NCTC-1469 cells.

Methods: C57BL/6J mice were fed with methionine and choline-deficient (MCD) diet and administered simultaneously with GPAE (500 and 1000 mg/kg/d, respectively) by gavage for six weeks. The biomarkers of NASH in serum and liver were determined. NCTC-1469 cells were pretreated with 0.25 mmol/L palmitic acid (PA) plus 0.5 mmol/L oleic acid (OA) for 24 h or treated with adenovirus expressing short-hairpin RNA against CFLAR (Ad-shCFLAR) for 24 h and then treated with GPAE (80 and 160 μg/mL, respectively) for 24 h, and the content of cellular biomarkers of NASH was detected.

Results: In mice treated with MCD, GPAE could decrease the levels of serum ALT, AST, the content of hepatic TG, TC and MDA, repress the activities and protein expression of CYP2E1 and CYP4A and the phosphorylation of JNK, increase the activities of HO-1, CAT and GSH-Px, up-regulate the mRNA expression of *PPARα, FABP5, CPT1α, ACOX, SCD-1, mGPAT, MTTP* and the protein expression of CFLAR and NRF2. In NCTC-1469 cells treated with PA and OA, GPAE could decrease the content of cellular TG and ROS, promote the uptake of 2-NBDG, up-regulate the protein expression of CFLAR and NRF2. In NCTC-1469 cells treated with Ad-sh*CFLAR*, GPAE up-regulated the mRNA and protein expression of CFLAR, down-regulated the phosphorylation of JNK, and increased the protein expression of NRF2 and pIRS1.

Conclusion: These results indicated that the activation on CFLAR-JNK pathway might be the main anti-NASH mechanism of GPAE, which on the one hand promote the β-oxidation and efflux of fatty acids in liver, and finally reduce hepatic lipid accumulation, on the other hand increase the activities of anti-oxidant enzymes and inhibit the activities of ROS generation enzymes by activating NRF2, and therefore attenuates hepatic oxidative stress damage.

1. Introduction

Nonalcoholic fatty liver disease (NAFLD) is a metabolic syndrome in which excessive fat accumulates in liver of patients who does not have a history of alcohol abuse (Angulo, 2002). NAFLD is an increasing prevalent health problem that ranges from simple fatty infiltration of liver parenchyma to steatosis with inflammation and hepatocellular ballooning (nonalcoholic steatohepatitis, NASH) and ultimately cirrhosis (Basaranoglu, Basaranoglu & Senturk, 2013). It is generally believed that the first stage of NAFLD/NASH is excessive fat accumulation of hepatic parenchymal cells, the second stage is hepatic inflammatory reaction and fibrosis (Day & James, 1998). At present, there is no effective drug for clinical treatment of NASH. The alternative therapies include lifestyle changes (such as changing the diet structure, increasing physical exercise) (Promrat et al., 2010), clinical application of anti-oxidant (Bell et al., 2012), insulin sensitizer (Sofer, Boaz, Matas, Mashavi & Shargorodsky, 2011), lipid-lowering drugs (Karahashi et al., 2013) and antidiabetic agents (Cariou et al., 2013).

Gynura procumbens (Lour.) Merr. is a Compositae plant, mainly distributed in Southeast Asia, especially in Malaysia, Indonesia and Thailand, as well as in Guangdong, Hainan, Guizhou and Yunnan of China. It is reported that *G. procumbens* has the

* Corresponding authors.
E-mail addresses: cy101610@qq.com (Y. Chen), 1597114874@qq.com (F.-m. Han).
[1] Both authors contributed equally to this work.

https://doi.org/10.1016/j.chmed.2019.09.005
1674-6384/

pharmacological activities against diabetes (Hassan, Yam, Ahmad & Yusof, 2010), hypertension (Hoe, Lee, Mok, Kamaruddin & Lam, 2011), cancer (Nisa, Hermawan, Murwanti & Meiyanto, 2012), inflammation (Iskander, Song, Coupar & Jiratchariyakul, 2002), kidney disease (Tan, Chan, Pusparajah, Lee & Goh, 2016), acute and chronic ethanol-induced liver steatosis (Li et al., 2015) and so on. *G. procumbens* aqueous extract (GPAE) prepared by extracting from its leaves with water and spray drying contains a variety of organic acids such as chlorogenic acid, protocatechuic acid, *p*-coumaric acid and caffeic acid and flavonoids such as apigenin, quercetin, rutin, myricetin and kaempferol (Kaewseejan, Sutthikhum & Siriamornpun, 2015). So far, it is not clear whether GPAE has a preventive and therapeutic effect on NASH.

The mice fed with methionine- and choline-deficient (MCD) diet lost weight due to reduced caloric intake, which is incontrast to humans with NASH who are mostly obese, indicating species differences between mice fed by MCD diet and humans with NASH (Schattenberg & Galle, 2010). However, mice and rats fed by MCD diet are the commonly used models for studying the inflammation and oxidative stress associated with NASH (London & George, 2007; Park et al., 2013). In the present work, the effect of GPAE on NASH and its underlying mechanism involved hepatic lipid metabolism and oxidative stress were investigated in mice fed by MCD diet and orally administered simultaneously with GPAE and in mice normal liver cell line NCTC-1469 which were pretreated with oleic acid (OA) plus palmitic acid (PA), and adenovirus expressing short-hairpin RNA against Caspase 8 and Fas-associated protein with death domain-like apoptosis regulator (Ad-shCFLAR), respectively.

2. Materials and methods

2.1. G. procumbens aqueous extract (GPAE)

GPAE was purchased from Shanxi Jintai Biol, China (Lot No. JT161115). In our previous study, the content of flavonoids and organic acids in GPAE was determined by LC-MS/MS method (Table 1) (You et al., 2017). The LC-MS/MS system was consisted of a LC-20AD parallel pump, a SIL-20A autosampler, a DGU-20A3R degasser unit, a CTO-20A column oven and a MS-8040 spectrometer (Shimadzu, Japan). Chromatographic separation was carried out on a shim-pack ODS column (4.6 μm, 150 mm × 2.0 mm i.d. Shimadzu) fitted with a guard column (4.6 μm, 150 mm × 2.0 mm i.d.) at a column temperature of 35 °C. A mixture of solvent A (0.1% formic acid in water) and solvent B (methanol) was used as the mobile phase at a flow rate of 0.2 mL/min under gradient elution program as follows: 0–14 min, linear gradient from 20% B to 85% B; 14.0–14.01 min, linear gradient from 85% B to 20% B; 14.01–20 min, holding at 20% B. Injection volume was 5 μL. The MS was set in positive multiple reaction monitoring (MRM) mode and the tuning parameters were optimized using the standard of analytes as follows: ion source gas 3 L/min curtain gas 15 L/min; ion spray voltage, −3.5 kv: temperature, 400 °C. Fig. 1 was the typical LC-MS/MS chromatogram of GPAE.

2.2. Animal and experimental protocols

Male C57BL/6J mice at 6 weeks of age (purchased from the disease prevention and control center of Hubei Province, certificate number: SCXK 2011-0012) were maintained in SPF animal room at temperature (22 ± 2) °C, (60 ± 5)% humidity and 12/12 h day/night cycle. Food and water were provided *ad libitum*. MCD diet and methionine- and choline-sufficient (MCS) diet were purchased from Nantong Trophy Feed Tech, China (Lot No. TP3005G for MCD and Lot No. TP3005GS for MCS). Both of diets contained the similar nutrients (corn oil, amino acid premixes, sucrose, starch, cellulose, vitamins, minerals, sodium bicarbonate) and anti-oxidants (TBHQ), whereas MCS diet contains 8 g/kg methionine and 2 g/kg choline, and MCD diet does not contain methionine and choline. Mice were randomly divided into four groups ($n = 8$ per group): normal control group (fed by MCS diet, named as NC group), model control group (fed by MCD diet, named as MC group), GPAE (dissolved in distilled water) group (fed by MCD diet, and simultaneously administered by gavage with GPAE at the dose of 500 and 1000 mg/kg once a day, respectively). All groups were given the same calorie intake to exclude the effect caused by different caloric and nutrient intake, and treated as stated as the above for six weeks. Then mice were fasted for 12 h with free access to water, the blood was respectively collected by extirpating eyeballs of the mice and the serum was separated from the blood. The fresh liver of mice was taken and weighed, the part of right liver lobe of each mouse was cut and fixed in 4% paraformaldehyde for the histological analysis, the residual liver was divided into three parts: one part for the preparation of liver S9 to measure the activities of CYP2E1 and 4A, one part for RT-qPCR and Western blotting, and one part for the determination of hepatic biochemical indicators. All efforts were made to minimize pain or discomfort of the animals. The handlings of animal were approved by Ethic Committee for Scientific Research of Hubei University, and were performed in accordance with the institutional guidelines for the care and use of laboratory animals.

2.3. Histological analysis

Liver specimens were fixed in 4% paraformaldehyde solution and embedded in paraffin, and cuted into 5 μm sections. Then, hematoxylin and eosin (H&E) staining, masson's trichrome (MT) staining and Oil-red O staining were performed, respectively. The histopathology of liver in the tested mice was observed under light microscope (Olympus, Tokyo, Japan) for the degree of hepatic steatosis and inflammatory reaction according to the validated histological scoring system recommended by the Pathology Committee of the NASH Clinical Research Network (Kleiner et al., 2005).

Table 1
Retention time, MS transitions and content of major active ingredients in GPAE.

Peaks	t_R/min	MS transitions (*m/z*)	Compounds	Content/(mg · kg^{-1})
1	5.26	153.0→109.0	Protocatechuate acid	95.7
2	6.97	353.0→191.1	Chlorogenic acid	39.1
3	8.04	179.0→135.05	Caffeic acid	18.8
4	9.76	163.0→119.1	p-coumaric acid	75.1
5	11.00	609.0→300.0	Rutin	22.0
6	11.97	317.0→151.0	Myricetin	23.0
7	13.41	301.0→151.0	Quercetin	27.0
8	14.61	285.0→93.2	Kaempferol	22.8
9	14.78	269.0→117.2	Apigenin	1.0
IS	17.82	265.0→224.2	Honokiol	0

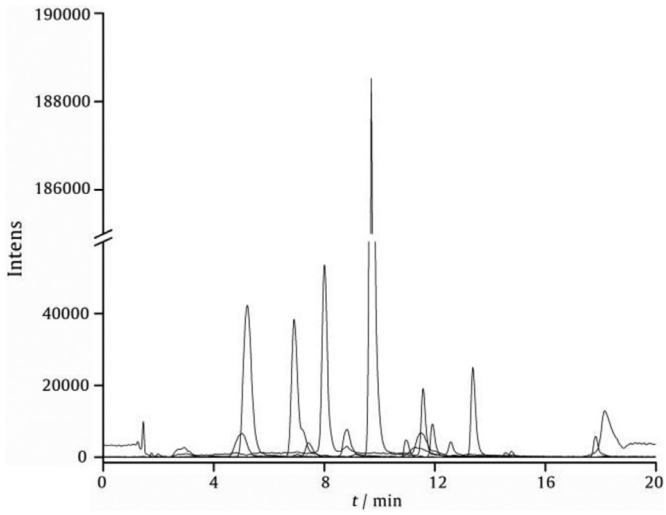

Fig. 1. 1 LC-MS/MS chromatogram of GPAE.

2.4. Determination of activities of CYP 2E1 and CYP 4A

Hepatic S9 was prepared freshly from the tested mice according to methods described previously (Zheng et al., 2014). Chlorzoxazone (CHZ; TRC, Canada) and lauric acid (LA; Nu-Chek Prep, USA) were used as the probe substrates of CYP2E1 and CYP4A, respectively. The production of 6-OH CHZ (TRC, Canada) and 12-OH LA (Sigma, USA) in liver S9 was used to evaluate the activities of hepatic CYP2E1 and CYP4A, respectively. All incubations were performed at 37 °C for 20 min in 200 μL potassium phosphate buffer (0.1 mol/L, pH 7.4) containing 5 mmol/L $MgCl_2$, 0.6 mg/mL (CYP2E1) or 0.5 mg/mL (CYP4A) of liver S9, 1 mmol/L NADPH and 50 μmol/L CHZ or 100 μmol/L LA. The incubation was terminated by adding cold ethyl acetate (800 μL) containing internal standard (IS) 4′-hydroxytolbutamide (TRC, Canada; 0.08 and 0.72 μmol/L for CYP2E1 and CYP4A, respectively). After the protein precipitation, the supernatant was evaporated at 30 °C and the residue was dissolved in 100 μL mobile phase. The LC–MS/MS system was the same as that of the determination of GPAE. 6-OH CHZ was separated on Shim-pack ODS C_{18} column (150 mm × 2.0 mm, 4.6 μm) using the mobile phase of mixed water (containing 0.1% formic acid) (A)-acetonitrile (B) at gradient elution program (0–5 min, 30%–85% B; 5–6 min, 85% B; 6–6.01 min, 85%–30% B; 6.01–11 min, 30% B; a flow rate of 0.2 mL/min), and detected by negative ion MRM with *m/z* 184.0→120.1 for 6-OH CHZ and 285.0→186.1 for IS. 12-OH LA was separated on the above stated column and the mobile phase by gradient elution (0–4 min, 25%–90% B; 4–8 min, 90% B; 8–8.01 min, 90%–25% B, 8.01–13 min, 25% B; a flow rate of 0.3 mL/min), and detected by negative ion selective ion monitoring with *m/z* 215.0 for 12-OH LA and 184.0 for IS. The column temperature was 40 °C.

2.5. Cell culture and treatment

Mice normal liver cell line NCTC-1469 was purchased from Hangzhou Haisheng Biotechnology Company. NCTC-1469 cells were cultured at 37 °C with 5% CO_2 in Dulbecco's Modified Eagle's medium (DMEM) (Gibco, USA) supplemented with 100 μg/mL streptomycin plus 100 U/mL penicillin (Hyclone, China) and 10% fetal bovine serum (FBS) (Gibco, USA).

NCTC-1469 cells pretreated with palmitic acid (PA; Sigma, USA) plus oleic acid (OA; Aladdin, China) in 6-well plates were divided into four groups: control group (treated with cell culture medium), model group (pretreated with 0.25 mmol/L PA (dissolved in distilled water) and 0.5 mmol/L OA (dissolved in methanol) for 24 h); GPAE (dissolved in distilled water) group (pretreated with PA and OA for 24 h, and then treated with GPAE (80 and 160 μg/mL, respectively) for 24 h).

NCTC-1469 cells transfected with Ad-shCFLAR in 12-well plates were divided into four groups: control group (treated with adenoviruses expressing shRNA against luciferase (Ad-shCtrl)); model group (infected with Ad-shCFLAR at 100 plaque-forming units (PFU)/cell for 24 h); GPAE (dissolved in distilled water) group (pretreated with Ad-shCFLAR for 24 h, and then treated with GPAE (80 and 160 μg/mL, respectively) for 24 h). ShRNA-encoding DNA sequences were synthesized and constructed into adenovirus plasmids by Haisheng Biological Technology Co., Ltd. The sequences of shRNA against CFLAR were: F-5'-GGGAAGAGTGTCTTGATGAA GATTCAAGAGATCTTCATCAAGACACTCTTCCTTTTTTG-3'; R-5'-GATCC AAAAAAGGAAGAGTGTCTTGATGAAGATCTCTTGAATCTTCATCAAGACA CTCTTCCCTGCA-3'.

2.6. Cytotoxicity analysis

The cytotoxicity of GPAE on NCTC-1469 cells was measured by the 3-[4,5-dimethylthiazol-2-yl]−2,5-diphenyltetrazolium bromide (MTT) (Sigma, USA) assay. Briefly, 1×10^3 NCTC-1469 cells were inoculated and adhered to the 96-well plates, and treated with different concentrations (0–160 μg/mL) of GPAE (dissolved in distilled water) at 37 °C for 24 h, 48 h and 72 h, respectively. Then 20 μL MTT (5 mg/ mL) and 180 μL PBS were added into each well for 4 h, the culture media in the plate was abandoned, and 150 μL DMSO was added to each well to dissolve the purple crystal. Finally, the absorbance of each well was detected at 570 nm using a microplate reader (BIO-RAD, USA).

2.7. Biochemical analysis

The levels of alanine aminotransferase (ALT), aspartate aminotransferase (AST), total cholesterol (TC), triglyceride (TG), HDL-C, LDL-C, malondialdehyde (MDA), catalase (CAT), glutathione peroxidase (GSH-Px) and heme oxygenase 1 (HO-1) in the C57BL/6J samples were determined by using commercially available kits according to the manufacturer's instructions (Nanjing Jiancheng Bio, China). The levels of cellular TG were measured using a cellular TG detection kit (Applygen, China) and the levels of cellular ROS were measured using a cellular ROS detection kit (Beyotime, China) according to the manufacturer's instructions after NCTC-1469 cells were pretreated with OA plus PA and subsequently treated with GPAE.

2.8. Glucose uptake analysis

After pretreatment with PA plus OA for 24 h and then treatment with GAPE (80 and 160 μg/mL) for 24 h, NCTC-1469 cells were incubated in glucose-free DMEM (Hyclone, USA) containing 50 μmol/L 2-(*N*-(7-nitrobenz-2-oxa-1,3-diazol-4-yl) amino)−2-deoxyglucose (2-NBDG; Invitrogen, USA) for 30 min. The fluorescent intensity was measured using a multimode microplate reader (Berthold TriStar LB941, USA) at excitation/emission wavelengths of 485/535 nm. The protein concentration of each well was detected by BCA kit (Thermo, USA) to normalize the data.

2.9. Real-Time quantitative PCR (RT-qPCR)

Total RNA were extracted from 50–100 mg frozen liver samples or 10^6 NCTC-1469 cells using 1 mL of Trizol reagent (Invitrogen, USA) plus 200 μL of chloroform. Agarose gel electrophoresis was performed to detect 28S, 18S and 5S bands for the integrity analysis of RNA. The absorbance ratio of 260 and 280 nm was detected by spectrophotometry for the purity analysis of RNA. Total RNA

(2 μg) was reverse transcribed into cDNA with Reverse transcription Kit (Toyobo, Japan) and used as the template of RT-qPCR. SYBR Green I fluorescent quantitative PCR Kit (Bio-Rad, USA) was used to detect the mRNA expression of the analyzed genes in liver tissue using β-actin as the internal reference. RT-qPCR were performed in CFX Connect™ Real-Time System (BIO-RAD, USA) for 40 cycles at the following conditions: pre-degeneration at 95 °C for 5 min, degeneration at 95 °C for 30 s, annealing at 58.3 °C for 30 s, extended at 72 °C for 30 s. Primers for the RT-PCR of each gene were listed in Table 2.

2.10. Western blotting

A total of 0.1 g of liver tissue from each mouse or 5×10^6 NCTC-1469 cells were homogenized in ice-cold 500 μL of RIPA lysate (Beyotime, China) containing PMSF (Beyotime, China), Cocktail (Roche, USA) and Phosphatase inhibitor (Roche, USA). Protein (50 μg) were separated by SDS-PAGE (5% concentrated gel and 10% separation gel) and electro-transferred onto PVDF membrane, which were then blocked for 2 h at room temperature and probed with the primary antibodies against CFLAR (1:1000; Shenyang Wanlei, China), c-Jun N-terminal kinase (JNK; 1:500; Shenyang Wanlei, China), phosphorylation of c-Jun N-terminal kinase (pJNK; 1:500; Shenyang Wanlei, China), nuclear factor erythroid 2-related factor 2 (NRF2; 1:500; Shenyang Wanlei, China), CYP2E1 (1:1000; Wuhan Boster Bio, China), CYP4A (1:1000; Abcam, USA), insulin receptor substrate 1 (IRS1; 1:500; Shenyang Wanlei, China), phosphorylation of insulin receptor substrate 1 (pIRS1; 1:1000; Millipore, USA) and β-actin (1:1000; Santa, USA), respectively. Then membranes were incubated for 1 h at room temperature with the secondary antibodies horseradish peroxidase labeled goat anti-mouse IgG (H + L) (1:10 000; KPL, USA) for β-actin and horseradish peroxidase labeled goat anti-rabbit IgG (H + L) (1:10 000; KPL, USA) for the other primary antibodies. The immunoreactive bands were visualized by enhanced chemiluminescent liquid (Beyotime, China) and X-ray film exposure according to the manufacturer's instructions, and then quantified by using ImageJ software (US National Institutes of Health).

Table 2
Primer sequences used for RT-qPCR.

Genes	Primers	Sequences (5'→3')
β-actin	Forward	AACCGTGAAAAGATGACCCAGAT
	Reverse	CACAGCCTGGATGGCTACGTA
PPARα	Forward	CGGGAAAGACCAGCAACAAC
	Reverse	ATAGCAGCCACAAACAGGGA
FABP5	Forward	GGAAGGAGAGCACGATAACAAGA
	Reverse	GGTGGCATTGTTCATGACACA
CPT1α	Forward	TCCACCCTGAGGCATCTATT
	Reverse	ATGACCTCCTGGCATTCTCC
ACOX	Forward	CGGAAGATACATCCCGGAGACC
	Reverse	AAGTAGGACACCATACCACCC
SCD-1	Forward	TACTACAAGCCCGGCCTCC
	Reverse	CAGCAGTACCAGGGCACCA
mGPAT	Forward	CCATTGTGGAGGATGAAGTG
	Reverse	TGGATCGTGCCAGATAGGGA
MTTP	Forward	GCTAAGAAGCTGATAATGGGAGG
	Reverse	CCACTCTTGGAGAAACGGTCATA
CFLAR	Forward	CTGTGTCTGCCGAGGTCATTC
	Reverse	AGAGCAATTCAGCCAAGGTAGC

Note: ACOX, acyl-coenzyme a oxidas X; CPT1α, carnitine palmitoyl transferase 1α; FABP5, fatty acid-binding proteins 5; mGPAT, glycerol-3-phosphate acyltransferase; MTTP, microsomal triglyceride transfer protein; PPARα, peroxisome proliferator activated receptor α; SCD-1, stearoyl-coenzyme A desaturase-1.

2.11. Statistical analysis

Data are presented as mean ± standard deviation (SD). Statistical comparisons were made using one-way analysis of variance (ANOVA), followed by Tukey's test. Values were considered statistically significant at $P < 0.05$.

3. Results

3.1. Effects of GPAE on lipid content and liver injury in MCD treated mice

The levels of hepatic TC and TG in MC group were higher than those in NC group ($P < 0.01$). Compared to MC group, GPAE treatment dose-dependently decreased hepatic TC content by 29.4% and 65.2%, TG content by 25.7% and 31.4%, respectively (Table 3). The activities of serum ALT and AST in MC group were higher than those in NC group. GPAE treatment markedly reduced the activities of serum ALT and AST in dose-dependent manner as compared to MC group (Table 3). The results from H&E and Oil Red O staining indicated that a large number of fat droplets were observed among liver cells, accompanied by inflammatory cell infiltration and the ballooning degeneration of hepatocytes in MC group. GPAE treatment improved the above symptoms of liver to a certain extent (Fig. 2). Additionally, according to the results of MT staining, there was no significant change in liver fibrosis of the tested mice.

3.2. Effects of GPAE on hepatic oxidative stress in MCD treated mice

The effects of GPAE on hepatic oxidative stress of the tested mice were shown in Table 4. Compared to NC group, the activities of hepatic CAT, GSH-Px and HO-1 in MC group were decreased obviously ($P < 0.01$), and the activities of hepatic CYP 2E1 and CYP 4A, as well as hepatic MDA content in MC group were significantly increased ($P < 0.01$). Compared to MC group, GPAE treatment increased the activities of CAT, GSH-Px and HO-1 respective by 102.3%–129.4%, 42.1%–53.3% and 195.8%–261.9%, whereas decreased the levels of the hepatic MDA, CYP2E1 and CYP4A respective by 50.9%–55.1%, 27.7%–33.6% and 17.8%–28.4% (Table 4).

3.3. Effects of GPAE on hepatic mRNA expression of lipid metabolism-related genes in MCD treated mice

The effect of GPAE on the mRNA expression of hepatic lipid metabolism related genes in the tested mice were shown in Fig. 3. Compared to NC group, the mRNA expression levels of hepatic *PPARα, FABP5, ACOX, CPT-1α, SCD-1, mGPAT* and *MTTP* in MC group were markedly down-regulated ($P < 0.05$ or $P < 0.01$). Compared to MC group, GPAE treatment at low dose (500 mg/kg) significantly

Table 3
Levels of ALT, AST and lipids in tested mice (mean ± SD, $n = 8$).

Items	NC	MC	500 mg/kg GPAE	1000 mg/kg GPAE
Serum ALT (U/L)	8.58±1.13	41.42±9.38 $^{\#\#}$	18.78±5.05$^{\#\#}$ **	18.40±6.09 $^{\#\#}$ **
Serum AST (U/L)	21.37±3.98	40.32±6.23 $^{\#\#}$	30.20±9.13$^{\#}$ *	21.97±8.79**
Hepatic TC (mmol/gprot)	0.09±0.01	0.17±0.04 $^{\#\#}$	0.12±0.05$^{\#}$ *	0.06±0.02**
Hepatic TG (mmol/gprot)	0.14±0.03	0.35±0.03 $^{\#\#}$	0.26±0.10$^{\#}$ *	0.24±0.02$^{\#}$ **

$^{\#}P < 0.01$ and $^{\#\#}P < 0.01$ MC *vs* NC, GPAE *vs* NC. $^{*}P < 0.05$ and $^{**}P < 0.01$ GPAE *vs* MC.

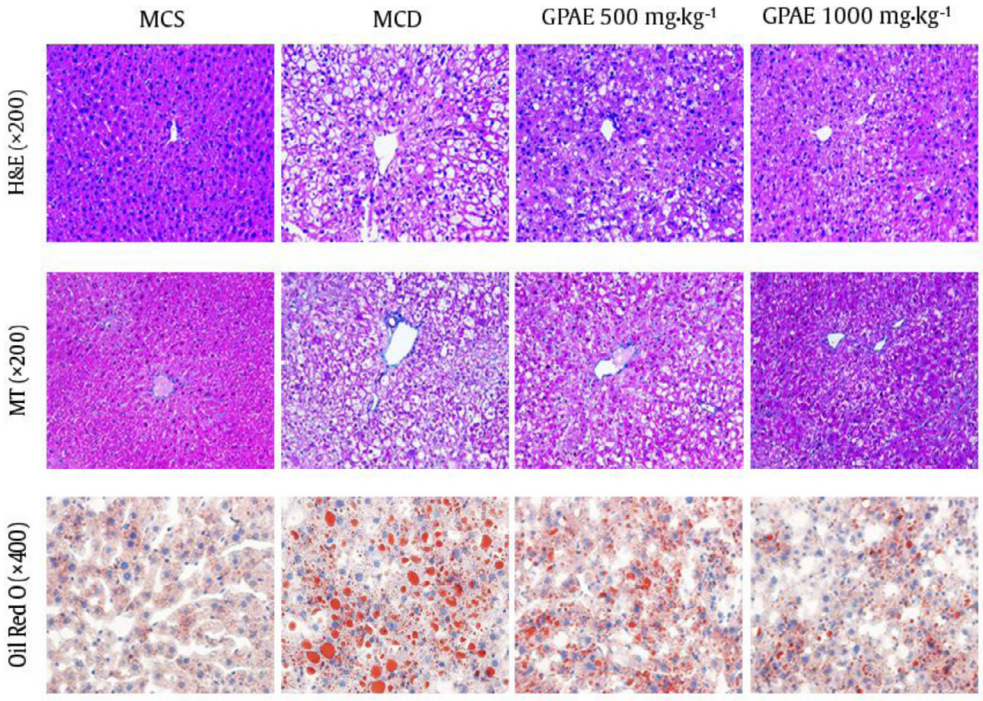

Fig. 2. Histological analysis of liver tissue by H&E, MT and Oil Red O in C57BL/6J.

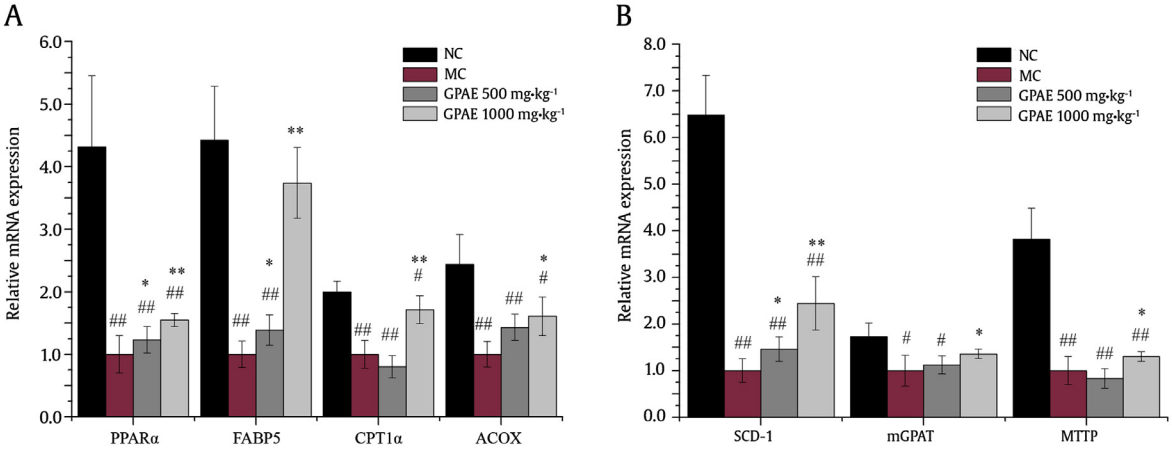

Fig. 3. Effects of GPAE on mRNA expression of hepatic lipid metabolism-related genes in C57BL/6J. The mRNA expression of PPARα, FABP5, CPT1α, ACOX (A) and SCD-1, mGPAT, MTTP (B) were analyzed by RT-qPCR after treatment of MCD and GPAE in C57BL/6J for six weeks (means ± SD, $n = 8$). $^{\#}P < 0.01$ and $^{\#\#}P < 0.01$ MC *vs* NC, GPAE *vs* NC. $^{*}P < 0.05$ and $^{**}P < 0.01$ GPAE *vs* MC.

up-regulated the mRNA expression levels of hepatic *PPARα*, *FABP5* and *SCD-1* ($P < 0.05$ or $P < 0.01$), and at high dose (1000 mg/kg) significantly up-regulated the mRNA expression levels of hepatic *PPARα*, *FABP5*, *ACOX*, *CPT-1α*, *SCD-1* and *MTTP* ($P < 0.05$ or $P < 0.01$).

3.4. Effects of GPAE on NASH-related protein expression in MCD treated mice

Compared to NC group, the protein levels of hepatic CFLAR and NRF2 were obviously decreased ($P < 0.05$ or $P < 0.01$), while the

Table 4
Activities of hepatic CYP 2E1 and CYP 4A in tested mice (mean ± SD, $n = 8$).

Items	NC	MC	500 mg/kg GPAE	1000 mg/kg GPAE
CYP2E1 (nmol/mgprotein/min)	0.19±0.05	0.31±0.04 $^{\#\#}$	0.22±0.02 **	0.20±0.05 **
CYP4A (nmol/mgprotein/min)	0.16±0.04	0.24±0.03 $^{\#\#}$	0.19±0.06 $^{\#*}$	0.17±0.06 *
Hepatic MDA (nmol/mgprot)	0.91±0.24	6.15±1.48 $^{\#\#}$	3.02±0.49 $^{\#\#**}$	2.76±0.99$^{\#\#**}$
Hepatic CAT (U/mgprot)	22.56±2.42	8.98±1.22 $^{\#\#}$	18.22±2.39**	20.6±4.53**
Hepatic GSH-Px (U/mgprot)	324.39±42.04	189.57±23.68 $^{\#\#}$	269.36±27.34**	290.61±20.80**
Hepatic HO-1 (ng/mL)	3.42±0.41	1.21±0.19 $^{\#\#}$	3.58±0.41**	4.38±0.11$^{\#**}$

$^{\#}P < 0.01$ and $^{\#\#}P < 0.01$ MC *vs* NC, GPAE *vs* NC. $^{*}P < 0.05$ and $^{**}P < 0.01$ GPAE *vs* MC.

protein levels of hepatic pJNK/JNK, CYP2E1 and CYP4A were significantly increased in MC group ($P < 0.05$ or $P < 0.01$) (Fig. 4). Compared to MC group, GPAE treatment at low dose (500 mg/kg) increased NRF2 protein level ($P < 0.05$), and no obvious effect was found for the protein expression of hepatic CFLAR, pJNK/JNK, CYP2E1 and CYP4A (Fig. 4). At the same time, GPAE treatment at high dose (1000 mg/kg) increased the protein levels of hepatic CFLAR and NRF2 ($P < 0.05$), and decreased the protein levels of hepatic *p*-JNK/JNK, CYP2E1 and CYP4A ($P < 0.05$).

3.5. Effects of GPAE on intracellular TG, ROS and 2-NBDG, and protein expression of CFLAR and NRF2 in OA plus PA pretreated NCTC-1469 cells

The effects of GPAE (0, 5, 10, 20, 40, 80 and 160 μg/mL) on the viability of NCTC-1469 cells at 24, 48 and 72 h were shown in Fig. 5A. GPAE treatment at the concentrations of 80 and 160 μg/mL had no significantly effect on the viability of the pretreated NCTC-1469 cells, so 80 and 160 μg/mL of GPAE were chosen in subsequent experiments.

The effects of GPAE on the cellular TG were shown in Fig. 5C and the results indicated that TG in model group was four times higher than that of control group. Treatment with GPAE at 80 and 160 μg/mL decreased TG content to 90% and 78% of model group, respectively. The results of ORO staining (Fig. 5B) were consistent with the content determination of TG.

The effects of GPAE on the cellular ROS (Fig. 5D) and 2-NBDG (Fig. 5E) showed that the pretreatment by OA plus PA increased the content of ROS and decreased the uptake of 2-NBDG in NCTC-1469 cells, the followed GPAE treatment for 24 h decreased the ROS content and increased the uptake of 2-NBDG in a dose-dependent manner.

Fig. 5F and H showed the effect of GPAE treatment on protein expression of CFLAR and NRF2 in OA+PA pretreated NCTC-1469 cells. Compared with control group, OA+PA pretreatment down-regulated the expression of CFLAR and NRF2, while GPAE-treatment for 24 h up-regulated the expression of CFLAR and NRF2 in a dose-dependent manner.

3.6. Effects of GPAE on expression of CFLAR-JNK pathway-related genes in NCTC-1469 cells transfected with Ad-shCFLAR

After NCTC-1469 cells being transfected with Ad-shCFLAR for 24 h, which were treated with GPAE for 24 h, the effects of the above treatment on the expression of CFLAR and NRF2, as well as the phosphorylation of JNK and IRS1, were shown in Fig. 6. Compared with control group, Ad-shCFLAR treatment down-regulated the mRNA and protein expression of CFLAR, increased the pJNK/JNK and down-regulated the protein expression of NRF2 and pIRS1. Whereas GPAE treatment promoted the mRNA and protein expression of CFLAR, decreased the protein expression of pJNK/JNK, and up-regulated the protein expression of NRF2 and pIRS1 in a dose-dependent manner.

4. Discussion

The histological features of NASH include evidence of steatosis, liver cell injury, mixed inflammatory lobular infiltrate, and different degrees of fibrosis (Basaranoglu et al., 2013). CFLAR is a member of the body's innate immune regulatory network and has a regulatory role in hepatocyte apoptosis and cellular immunity (Kohl et al., 2013; Schattenberg et al., 2011). It is reported that CFLAR could ameliorate NASH by inhibiting the phosphorylation of JNK (Wang et al., 2017). The CFLAR-knockout mice showed markedly increased glucolipid metabolism and oxidative stress disorder, inflammatory responses and fibrosis, which were significantly improved or even reversed by over-expressing CFLAR in mice (Schattenberg et al., 2012; Wang et al., 2017). Our result is consistent with the above reported literature, suggesting that GPAE can relieve NASH by activating CFLAR, and inhibiting the expression of its downstream p-JNK/JNK. There are some targets located in the downstream of JNK, which can regulate lipid metabolism, insulin resistant and oxidative stress (Kohl et al., 2013; Leamy, Egnatchik & Young, 2013; Schattenberg et al., 2011; Wang et al., 2017). Therefore, we further studied the regulation mechanism of GPAE on hepatic lipid metabolism, insulin resistant and oxidative stress *in vivo* and *in vitro*.

One of the major pathological changes in NAFLD/NASH is hepatic steatosis, which may be associated with decreased fatty acid oxidation in liver (Browning & Horton, 2004). PPARα plays a central role in the process of fatty acid β-oxidation. Its expression level has an important regulatory effect on NASH of rodents induced by eating MCD or high-fat diet (Abdelmegeed et al., 2011). CPT1α and ACOX are the key speed-limiting enzymes of fatty acid β-oxidation, and regulated by PPARα (Wang et al., 2016). FABPS5 is a necessary condition for the use of long-chain fatty acids in liver (Furuhashi & Hotamisligil, 2008). Our results showed that GPAE significantly promoted the mRNA expression of *PPARα, FABPS5,*

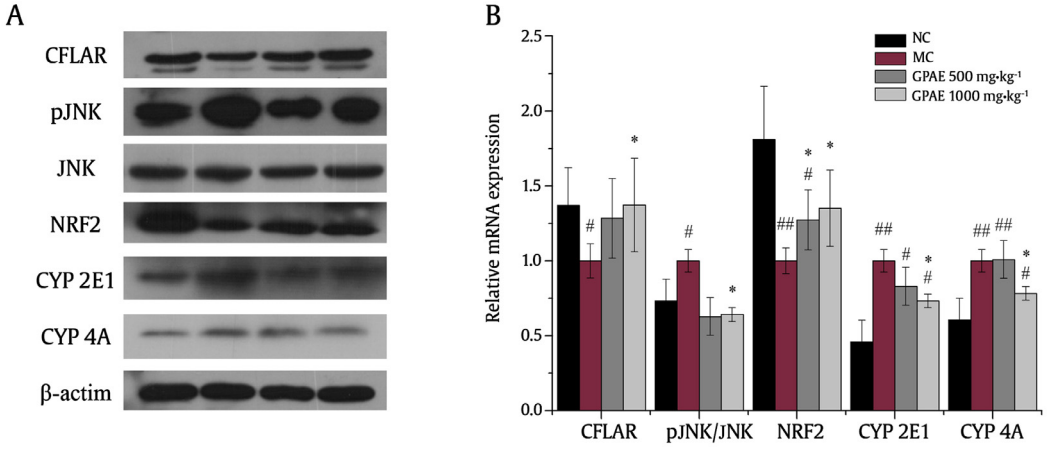

Fig. 4. Effects of GPAE on NASH-related protein expression in liver of tested mice. Protein expression of CFLAR, pJNK, NRF2, CYP2E1, CYP4A were analyzed by Western blotting after treatment of MCD and GPAE in C57BL/6J for six weeks (means ± SD, $n = 8$). $^{\#}P < 0.05$ and $^{\#\#}P < 0.01$ MC *vs* NC, GPAE *vs* NC. $^{*}P < 0.05$ and $^{**}P < 0.01$ GPAE *vs* MC.

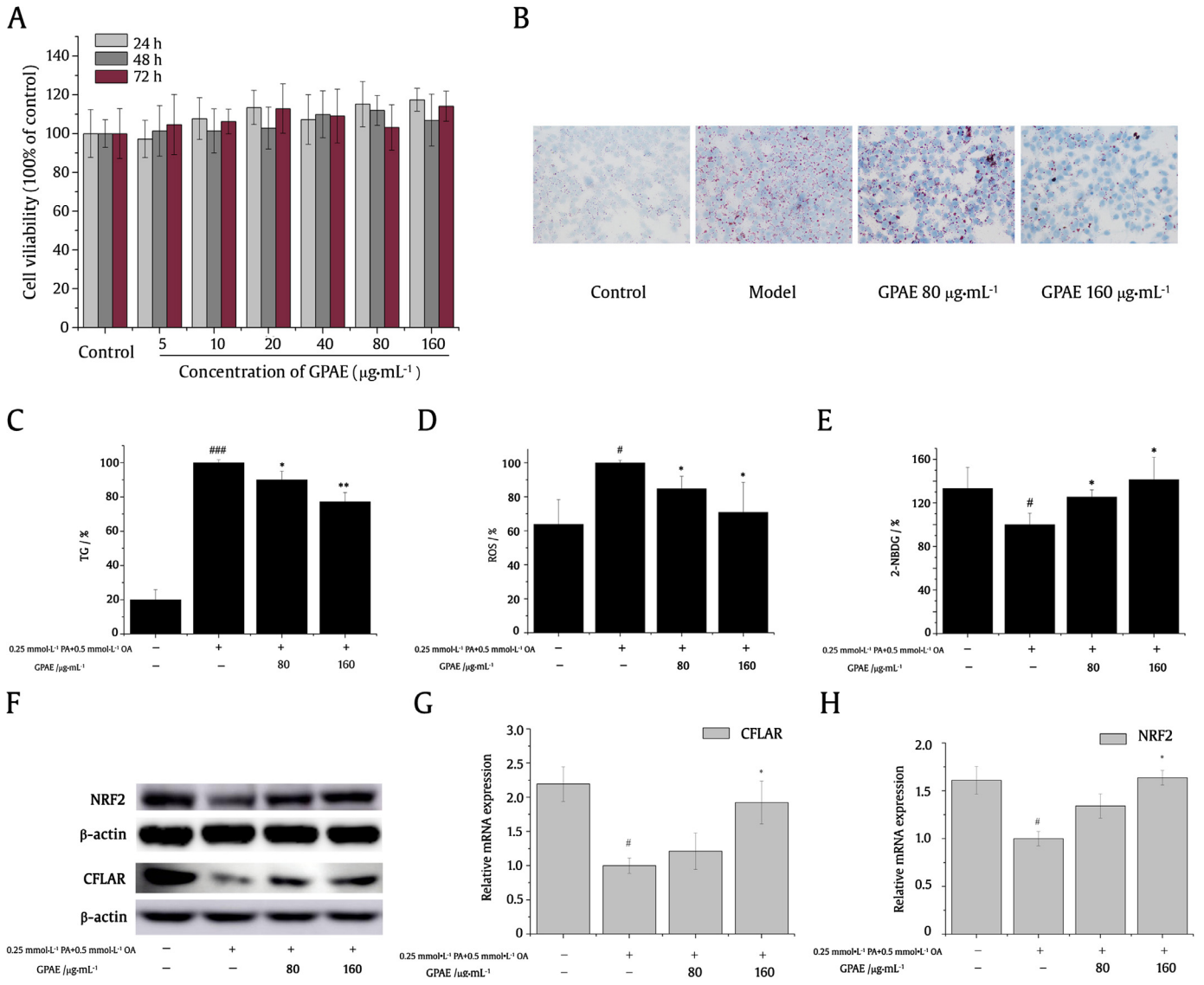

Fig. 5. Effects of GPAE on NASH-related targets in PA plus OA pretreated NCTC-1469 cells. Cellular viability (A), Oil-red O staining (B), cellular TG (C), cellular ROS (D), 2-NBDG (E), protein expression of CFLAR (F, G) and NRF2 (F, H) in NCTC-1469 cells after OA plus PA pretreated for 24 h and GPAE (80 and 160 μg/mL, respectively) treatment for 24 h were measured. Results represent average of three independent experiments in triplicates. Data are means ± SD. $^{\#}P < 0.05$ and $^{\#\#}P < 0.01$ *vs* control group. $^{*}P < 0.05$ and $^{**}P < 0.01$ *vs* model group, respectively.

CPT1α and *ACOX* in the liver of NASH model mice, suggesting that the decreased hepatic fatty acid accumulation induced by GPAE may be associated with the up-regulating expression of ACOX and CPT1α by activating PPARα, and therefore accelerating fatty acid β-oxidation in liver.

The impairment in the esterification process of saturated fatty acids will cause marked increase in hepatocellular apoptosis, inflammation, and insulin resistance (Lockman & Nyirenda, 2010). High exposure of free fatty acids leads to cytotoxicity and must be incorporated into complex lipids, such as phospholipids, cholesterol esters and TG (Ducheix et al., 2016). SCD-1 is a critical enzyme which is responsible for converting saturated fatty acids to TG (Lockman & Nyirenda, 2010). mGPAT is involved in the synthesis of TG by the esterification of free fatty acids (Ducheix et al., 2016). MTTP is responsible for transporting TG out of liver in the form of VLDL (Hussain, Shi & Dreizen, 2003). It was reported that MCD diet caused hepatic lipid accumulation by reducing the formation of VLDL (Fast & Vance, 1995; Marcolin et al., 2011) in liver and the expressions of hepatic SCD-1, mGPAT and MTTP in mice with NASH were significantly inhibited (Chang et al., 2010; Rizki et al., 2006; Zhang et al., 2012). The results of this study suggested that the up-regulated mRNA expression of hepatic *SCD-1, mGPAT* and *MTTP* may be another important way for GPAE to reduce hepatic lipid accumulation of mice with NASH.

NRF2 is a key regulatory factor in the anti-oxidant signaling pathway and plays an important role in regulating oxidative stress damage (Vomund, Schafer, Parnham, Brune & von Knethen, 2017). It was reported that NRF2 expression was decreased, and NASH symptoms aggravated in mice fed MCD diet for two weeks (Chowdhry et al., 2010). CAT, GSH-Px and HO-1 are the important enzymes for scavenging free radicals in the organism, which can alleviate the lipid peroxidation of cell membranes (Rezazadeh, Yazdanparast & Molaei, 2012; Tariq, Green & Hodson, 2014). The activities of hepatic CYP4A and CYP2E1 in humans and rodents with fatty liver were higher than those in normal condition, which is an important factor in inducing wild mice to suffer from fatty

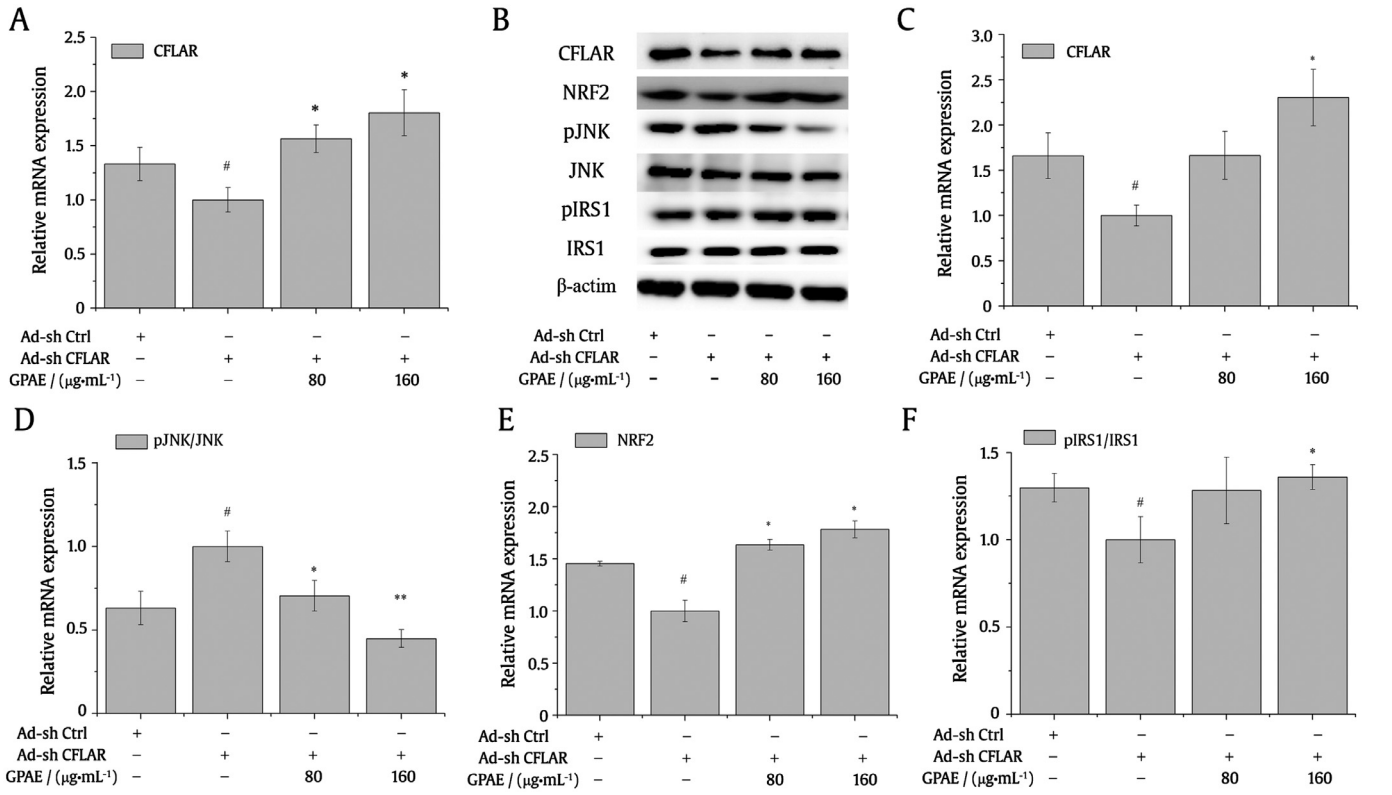

Fig. 6. Effects of GPAE on NASH-related targets in Ad-shCFLAR treated NCTC-1469 cells. The mRNA expression of CFLAR (A), protein expression of CFLAR (B, C), pJNK (B, D), NRF2 (B, E) and pIRS1 (B, F) in NCTC-1469 cells after Ad-shCFLAR treatment for 24 h and GPAE (80 and 160 μg/mL, respectively) treatment for 24 h were measured. Results represent the average of three independent experiments in triplicates. Data are means ± SD. $^{\#}P < 0.05$ and $^{\#\#}P < 0.01$ *vs* control group. $^{*}P < 0.05$ and $^{**}P < 0.01$ *vs* model group.

liver disease induced by feeding MCD diet (Leclercq et al., 2000; Weltman, Farrell, Hall, Ingelman-Sundberg & Liddle, 1998). And the content of hepatic MDA in humans and mice with NASH was also higher than those in normal condition (Koek, Liedorp & Bast, 2011). Our results showed that the levels of hepatic MDA, CYP2E1 and CYP4A in GPAE groups were significantly lower than those in MC group, and the levels of NRF2, CAT, GSH-Px and HO-1 were significantly higher than those in MC group, which indicated that GPAE could effectively improve the anti-oxidant ability and alleviate the oxidative stress injury of the liver in NASH model mice. In addition, serum AST and ALT levels are sensitive indicators for evaluating the degree of liver damage (Giboney, 2005). GPAE significantly reduced the activities of serum AST and ALT of mice fed by MC diet, also indicating the preventive effect of GPAE against NASH.

To confirm the effect of GPAE on NASH-related genes, we further studied the regulation mechanism of GPAE on hepatic lipid metabolism, insulin resistant and oxidative stress in NCTC-1469 cells treated by PA plus OA, and by Ad-shRNA mediated CFLAR knockdown. The results showed that GPAE treatment could decrease the cellular TG and ROS, increase the uptake of 2-NBDG and the protein expression of CFLAR and NRF2 in NCTC-1469 cells as compared with the PA plus OA pretreated group. Our results also revealed that GPAE treatment could rescue Ad-shRNA mediated CFLAR knockdown in NCTC-1469 cells. After the pretreatment with Ad-shCFLAR and the followed treatment with GPAE, the mRNA and protein expression of CFLAR, as well as the protein expression of NRF2 and pIRS1, were up-regulated, while the protein expression of pJNK was down-regulated as compared with Ad-shCFLAR treated group. The results in NCTC-1469 cells were consisted with the results *in vivo*, suggesting that GPAE could regulate the CFLAR-JNK pathway to ameliorate the lipid accumulation, insulin resistant and oxidative stress.

There are many natural active ingredients contained in GPAE, such as apigenin, quercetin, rutin, myricetin, chlorogenic acid, protocatechuate acid, *p*-coumaric acid, caffeic acid and kaempferol (You et al., 2017). A lot of literatures have been reported about the protective effects of these natural active ingredients on hepatic lipid degeneration and oxidative stress injury (Lee, Hsu, Lin, Kao & Wang, 2017; Wang, Chen, Hu & Yuan, 2014; Wang, Sun, Jiang, Xie & Zhang, 2015; Wu et al., 2011; Xia et al., 2016). Therefore we speculated that the observed anti-NASH activity is due to the combined effect of the active ingredients existed in GPAE.

5. Conclusion

To sum up, the speculated preventive mechanism of GPAE against NASH was shown in Fig. 7. GPAE could inhibite the phosphorylation of JNK by activating the expression of CFLAR, and then regulate the downstream genes of JNK related to lipid metabolism, oxidative stress and insulin resistance. For lipid metabolism, GPAE promoted hepatic lipid β-oxidation by up-regulating the expression of PPARα, FABP5, CPT1α and ACOX, promoted hepatic lipid efflux by up-regulating the expression of SCD-1, mGPAT and MTTP, and finally reduced hepatic lipid accumulation. For oxidative stress, GPAE promoted the activities of anti-oxidant enzymes (CAT, GSH-Px and HO-1) and inhibited the activities of ROS generation enzymes (CYP2E1 and CYP4A) by up-regulating NRF2 expression, and then reduce the hepatic oxidative stress damage. For insulin resistance, GPAE promoted the phosphorylation of IRS1, and then im-

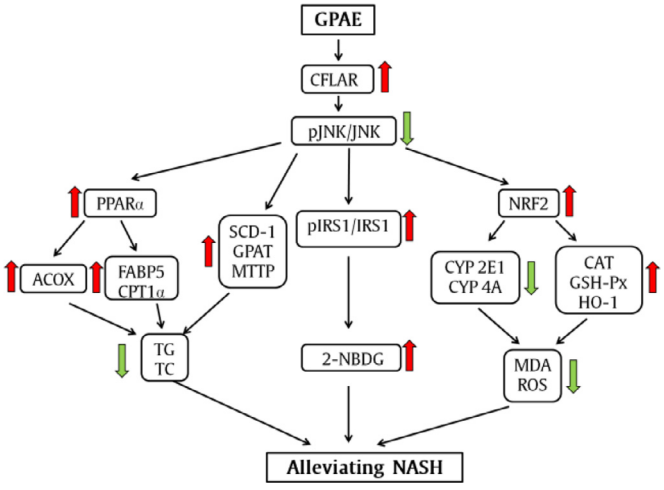

Fig. 7. Proposed mechanism of GPAE on NASH.

prove the hepatic insulin resistance to enhance the uptake of glucose in liver cells.

Declaration of Competing Interest

The authors declare no conflict of interest.

Acknowledgment

This study was supported by the major technological innovation project of Hubei Province (grant No. 2016ACA140) and the united fund for innovation and entrepreneurship of Ministry of Education of China (grant No. 201610512001).

References

Abdelmegeed, M. A., Yoo, S. H., Henderson, L. E., Gonzalez, F. J., Woodcroft, K. J., & Song, B. J. (2011). PPARalpha expression protects male mice from high fat-induced nonalcoholic fatty liver. *Journal of Nutrition, 141*(4), 603–610.

Angulo, P. (2002). Nonalcoholic fatty liver disease. *New England Journal of Medicine, 346*(16), 1221–1231.

Basaranoglu, M., Basaranoglu, G., & Senturk, H. (2013). From fatty liver to fibrosis: A tale of "second hit". *World Journal of Gastroenterology, 19*(8), 1158–1165.

Bell, L. N., Wang, J., Muralidharan, S., Chalasani, S., Fullenkamp, A. M., Wilson, L. A., et al. (2012). Relationship between adipose tissue insulin resistance and liver histology in nonalcoholic steatohepatitis: A pioglitazone versus vitamin e versus placebo for the treatment of nondiabetic patients with nonalcoholic steatohepatitis trial follow-up study. *Hepatology, 56*(4), 1311–1318.

Browning, J. D., & Horton, J. D. (2004). Molecular mediators of hepatic steatosis and liver injury. *Journal of Clinical Investigation, 114*(2), 147–152.

Cariou, B., Hanf, R., Lambert-Porcheron, S., Zair, Y., Sauvinet, V., Noel, B., et al. (2013). Dual peroxisome proliferator-activated receptor alpha/delta agonist GFT505 improves hepatic and peripheral insulin sensitivity in abdominally obese subjects. *Diabetes Care, 36*(10), 2923–2930.

Chang, X., Yan, H., Fei, J., Jiang, M., Zhu, H., Lu, D., et al. (2010). Berberine reduces methylation of the MTTP promoter and alleviates fatty liver induced by a high-fat diet in rats. *Journal of Lipid Research, 51*(9), 2504–2515.

Chowdhry, S., Nazmy, M. H., Meakin, P. J., Dinkova-Kostova, A. T., Walsh, S. V., Tsujita, T., et al. (2010). Loss of Nrf2 markedly exacerbates nonalcoholic steatohepatitis. *Free Radical Biology and Medicine, 48*(2), 357–371.

Day, C. P., & James, O. F. (1998). Steatohepatitis: A tale of two "hits"? *Gastroenterology, 114*(4), 842–845.

Ducheix, S., Vegliante, M. C., Villani, G., Napoli, N., Sabba, C., Moschetta, A., et al. (1995). Nascent VLDL phospholipid composition is altered when phosphatidylcholine biosynthesis is inhibited: Evidence for a novel mechanism that regulates VLDL secretion. *Biochimica et Biophysica Acta, 1258*(2), 159–168.

Furuhashi, M., & Hotamisligil, G. S. (2008). Fatty acid-binding proteins: Role in metabolic diseases and potential as drug targets. *Nature Reviews Drug Discovery, 7*(6), 489–503.

Giboney, P. T. (2005). Mildly elevated liver transaminase levels in the asymptomatic patient. *American Family Physician, 71*(6), 1105–1110.

Hassan, Z., Yam, M. F., Ahmad, M., & Yusof, A. P. (2010). Antidiabetic properties and mechanism of action of gynura procumbens water extract in streptozotocin-induced diabetic rats. *Molecules, 15*(12), 9008–9023. doi:10.3390/molecules15129008.

Hoe, S. Z., Lee, C. N., Mok, S. L., Kamaruddin, M. Y., & Lam, S. K. (2011). *Gynura procumbens* Merr. decreases blood pressure in rats by vasodilatation via inhibition of calcium channels. *Clinics (Sao Paulo), 66*(1), 143–150.

Hussain, M. M., Shi, J., & Dreizen, P. (2003). Microsomal triglyceride transfer protein and its role in apoB-lipoprotein assembly. *Journal of Lipid Research, 44*(1), 22–32.

Iskander, M. N., Song, Y., Coupar, I. M., & Jiratchariyakul, W. (2002). Antiinflammatory screening of the medicinal plant *Gynura procumbens*. *Plant Foods for Human Nutrition (Dordrecht, Netherlands), 57*(3–4), 233–244.

Kaewseejan, N., Sutthikhum, V., & Siriamornpun, S. (2015). Potential of *Gynura procumbens* leaves as source of flavonoid-enriched fractions with enhanced antioxidant capacity. *Journal of Functional Foods, 12*(4), 120–128.

Karahashi, M., Hoshina, M., Yamazaki, T., Sakamoto, T., Mitsumoto, A., Kawashima, Y., et al. (2013). Fibrates reduce triacylglycerol content by upregulating adipose triglyceride lipase in the liver of rats. *Journal of Pharmacological Sciences, 123*(4), 356–370.

Kleiner, D. E., Brunt, E. M., Van Natta, M., Behling, C., Contos, M. J., Cummings, O. W., et al. (2005). Design and validation of a histological scoring system for nonalcoholic fatty liver disease. *Hepatology (Baltimore, Md.), 41*(6), 1313–1321.

Koek, G. H., Liedorp, P. R., & Bast, A. (2011). The role of oxidative stress in non-alcoholic steatohepatitis. *Clinica Chimica Acta, 412*(15–16), 1297–1305.

Kohl, T., Gehrke, N., Schad, A., Nagel, M., Worns, M. A., Sprinzl, M. F., et al. (2013). Diabetic liver injury from streptozotocin is regulated through the caspase-8 homolog cFLIP involving activation of JNK2 and intrahepatic immunocompetent cells. *Cell Death & Disease, 4*, e712. doi:10.1038/cddis.2013.228.

Leamy, A. K., Egnatchik, R. A., & Young, J. D. (2013). Molecular mechanisms and the role of saturated fatty acids in the progression of non-alcoholic fatty liver disease. *Progress in Lipid Research, 52*(1), 165–174.

Leclercq, I. A., Farrell, G. C., Field, J., Bell, D. R., Gonzalez, F. J., & Robertson, G. R. (2000). CYP2E1 and CYP4A as microsomal catalysts of lipid peroxides in murine nonalcoholic steatohepatitis. *Journal of Clinical Investigation, 105*(8), 1067–1075.

Lee, Y. J., Hsu, J. D., Lin, W. L., Ka, S. H., & Wang, C. J. (2017). Upregulation of caveolin-1 by mulberry leaf extract and its major components, chlorogenic acid derivatives, attenuates alcoholic steatohepatitis via inhibition of oxidative stress. *Food & Function, 8*(1), 397–405.

Li, X. J., Mu, Y. M., Li, T. T., Yang, Y. L., Zhang, M. T., Li, Y. S., et al. (2015). *Gynura procumbens* reverses acute and chronic ethanol-induced liver steatosis through MAPK/SREBP-1c-dependent and -independent pathways. *Journal of Agricultural and Food Chemistry, 63*(38), 8460–8471.

Lockman, K. A., & Nyirenda, M. J. (2010). Interrelationships between hepatic fat and insulin resistance in non-alcoholic fatty liver disease. *Current Diabetes Reviews, 6*(5), 341–347.

London, R. M., & George, J. (2007). Pathogenesis of NASH: Animal models. *Clinics in Liver Disease, 11*(1), 55–74.

Marcolin, E., Forgiarini, L. F., Tieppo, J., Dias, A. S., Freitas, L. A., & Marroni, N. P. (2011). Methionine- and choline-deficient diet induces hepatic changes characteristic of non-alcoholic steatohepatitis. *Arquivos de Gastroenterologia, 48*(1), 72–79.

Nisa, F., Hermawan, A., Murwanti, R., & Meiyanto, E. (2012). Antiproliferative effect of *Gynura procumbens* (Lour.) Merr. leaves etanolic extract on 7,12-dimethylbenz(a)antracene induced male rat liver. *Advanced Pharmaceutical Bulletin, 2*(1), 99–106.

Park, H. J., Han, J. M., Kim, H. G., Choi, M. K., Lee, J. S., Lee, H. W., et al. (2013). Chunggan extract (CGX), methionine-and choline-deficient (MCD) diet-induced hepatosteatosis and oxidative stress in C57BL/6 mice. *Human & Experimental Toxicology, 32*(12), 1258–1269.

Promrat, K., Kleiner, D. E., Niemeier, H. M., Jackvony, E., Kearns, M., Wands, J. R., et al. (2010). Randomized controlled trial testing the effects of weight loss on nonalcoholic steatohepatitis. *Hepatology (Baltimore, Md.), 51*(1), 121–129.

Rezazadeh, A., Yazdanparast, R., & Molaei, M. (2012). Amelioration of diet-induced nonalcoholic steatohepatitis in rats by Mn-salen complexes via reduction of oxidative stress. *Journal of Biomedical Science, 19*, 26.

Rizki, G., Arnaboldi, L., Gabrielli, B., Yan, J., Lee, G. S., Ng, R. K., et al. (2006). Mice fed a lipogenic methionine-choline-deficient diet develop hypermetabolism coincident with hepatic suppression of SCD-1. *Journal of Lipid Research, 47*(10), 2280–2290.

Schattenberg, J. M., & Galle, P. R. (2010). Animal models of non-alcoholic steatohepatitis: Of mice and man. *Digestive Diseases (Basel, Switzerland), 28*(1), 247–254.

Schattenberg, J. M., Nagel, M., Kim, Y. O., Kohl, T., Worns, M. A., Zimmermann, T., et al. (2012). Increased hepatic fibrosis and JNK2-dependent liver injury in mice exhibiting hepatocyte-specific deletion of cFLIP. *American Journal of Physiology Gastrointestinal and Liver Physiology, 303*(4), G498–G506.

Schattenberg, J. M., Zimmermann, T., Worns, M., Sprinzl, M. F., Kreft, A., Kohl, T., et al. (2011). Ablation of c-FLIP in hepatocytes enhances death-receptor mediated apoptosis and toxic liver injury *in vivo*. *Journal of Hepatology, 55*(6), 1272–1280. doi:10.1016/j.jhep.2011.03.008.

Sofer, E., Boaz, M., Matas, Z., Mashavi, M., & Shargorodsky, M. (2011). Treatment with insulin sensitizer metformin improves arterial properties, metabolic parameters, and liver function in patients with nonalcoholic fatty liver disease: A randomized, placebo-controlled trial. *Metabolism, 60*(9), 1278–1284.

Tan, H. L., Chan, K. G., Pusparajah, P., Lee, L. H., & Goh, B. H. (2016). Gynura procumbens: An overview of the biological activities. *Frontiers in Pharmacology, 7*, 52. doi:10.3389/fphar.2016.00052.

Tariq, Z., Green, C. J., & Hodson, L. (2014). Are oxidative stress mechanisms the common denominator in the progression from hepatic steatosis towards non-alcoholic steatohepatitis (NASH)? *Liver International, 34*(7), e180–e190.

Vomund, S., Schafer, A., Parnham, M. J., Brune, B., & von Knethen, A. (2017). Nrf2, the master regulator of anti-oxidative responses. *International Journal of Molecular Sciences, 18*(12). doi:10.3390/ijms18122772.

Wang, C., Duan, X., Sun, X., Liu, Z., Sun, P., Yang, X., et al. (2016). Protective effects of glycyrrhizic acid from edible botanical *Glycyrrhiza glabra* against non-alcoholic steatohepatitis in mice. *Food & Function, 7*(9), 3716–3723.

Wang, E., Chen, F., Hu, X., & Yuan, Y. (2014). Protective effects of apigenin against furan-induced toxicity in mice. *Food & Function, 5*(8), 1804–1812.

Wang, M., Sun, J., Jiang, Z., Xie, W., & Zhang, X. (2015). Hepatoprotective effect of kaempferol against alcoholic liver injury in mice. *American Journal of Chinese Medicine, 43*(2), 241–254. doi:10.1142/s0192415x15500160.

Wang, P. X., Ji, Y. X., Zhang, X. J., Zhao, L. P., Yan, Z. Z., Zhang, P., et al. (2017). Targeting CASP8 and FADD-like apoptosis regulator ameliorates nonalcoholic steatohepatitis in mice and nonhuman primates. *Nature Medicine, 23*(4), 439–449.

Weltman, M. D., Farrell, G. C., Hall, P., Ingelman-Sundberg, M., & Liddle, C. (1998). Hepatic cytochrome P450 2E1 is increased in patients with nonalcoholic steatohepatitis. *Hepatology (Baltimore, Md.), 27*(1), 128–133.

Wu, C. H., Lin, M. C., Wang, H. C., Yang, M. Y., Jou, M. J., & Wang, C. J. (2011). Rutin inhibits oleic acid induced lipid accumulation via reducing lipogenesis and oxidative stress in hepatocarcinoma cells. *Journal of Food Science, 76*(2), 65–72.

Xia, S. F., Le, G. W., Wang, P., Qiu, Y. Y., Jiang, Y. Y., & Tang, X. (2016). Regressive effect of myricetin on hepatic steatosis in mice fed a high-fat diet. *Nutrients, 8*(12). doi:10.3390/nu8120799.

You, J. J., Peng, Z. H., Han, F. M., You, J. J., Peng, Z. H., & Han, F. M. (2017). Simultaneous determination of nine components in *Gynura procumbens* aqueous extract by hplc-ms/ms. *Chinese Traditional & Herbal Drugs, 48*(2), 294–298.

Zhang, B., Xue, C., Hu, X., Xu, J., Li, Z., Wang, J., et al. (2012). Dietary sea cucumber cerebroside alleviates orotic acid-induced excess hepatic adipopexis in rats. *Lipids in Health and Disease, 11*, 48. doi:10.1186/1476-511x-11-48.

Zheng, R., Dragomir, A. C., Mishin, V., Richardson, J. R., Heck, D. E., Laskin, D. L., et al. (2014). Differential metabolism of 4-hydroxynonenal in liver, lung and brain of mice and rats. *Toxicology and Applied Pharmacology, 279*(1), 43–52.